REPORTS OF PRACTICAL ONCOLOGY AND RADIOTHERAPY

A comprehensive site-specific analysis of patient-specific quality assurance based on dose volume histogram of RapidArc treatment delivery

Authors: A Sumanta Manna, Benoy Kumar Singh, K J Maria Das

A comprehensive site-specific analysis of patient-specific quality assurance based on dose volume histogram of RapidArc treatment delivery

Running Title: Site-Specific PSQA using DVH Analysis

A Sumanta Manna[1, 2], Benoy Kumar Singh[1], K J Maria Das[3]

[1]Department of Physics, GLA University, Mathura, Uttar Pradesh, India
[2]Specialty of Medical Physics, Kalyan Singh Super Specialty Cancer Institute, Lucknow, Uttar Pradesh, India
[3]Department of Radiotherapy, Sanjay Gandhi Postgraduate Institute of Medical Sciences, Lucknow, Uttar Pradesh, India

Corresponding Author: Sumanta Manna**,** Medical Physicist/Scientist-I**,** Specialty of Medical Physics**,** Kalyan Singh Super Specialty Cancer Institute, C G City, Lucknow, Uttar Pradesh 226002, India; e-mail: Sumanta7915@gmail.com

Abstract

Background: The current study aims to evaluate the use of dose-volume histogram (DVH) metrics as part of a comprehensive pre-treatment quality assurance (PSQA) protocol for RapidArc treatment delivery.

Materials and methods: A total of ninety patients were included in this study, with the patient population divided into four groups: Brain (n = 15), Head and Neck (H & N) (n = 30), Thorax (n = 15), and Pelvis (n = 30) RapidArc plans. The delivered dose was assessed using the Octavius 4D 1500 detector array and the Verisoft DVH application, focusing on DVH-related errors pertaining to targets and organ-at-risk (OARs). Additionally, three-dimensional local and global gamma passing rates were analyzed in the axial, coronal, and sagittal planes using various gamma criteria, including 3 mm/3%, 3 mm/2%, 2 mm/3%, and 2 mm/2%.

Results: All treatment plans met the action level requirement, achieving a gamma acceptance rate exceeding 95% with a 3%/3 mm criterion. Among the anatomical planes, the transverse plane consistently exhibited the highest passing rates for various global gamma criteria across all treatment sites. Local gamma analysis revealed that the coronal plane had the highest passing rates for thorax and pelvis sites compared to other planes. DVH analysis indicated that doses to target volumes remained within specified tolerances for all cases. The most significant OAR dose discrepancies were observed in the H&N region.

Conclusion: Integrating DVH metrics into the RapidArc PSQA protocol can yield clinically significant results closely aligned with the gamma index. It was observed that a single action-level approach cannot be universally applied to DVH metrics across different anatomical sites.

Keywords: gamma index; dose volume histogram; rapidArc, patient specific quality assurance; Octavius 4D

Introduction

Contemporary radiotherapy techniques are so intricate in planning and delivery phases that they necessitate pre-treatment quality assurance (PSQA) tailored to individual patients [1]. Current advanced radiation techniques such as IMRT/VMAT are known for their steep dose gradients, meaning even a minor error can substantially impact the outcomes. Moreover, with the increasing adoption of these state-of-the-art radiotherapy techniques, there is a growing focus on the verification of dosimetry and quality assurance (QA) [2].

The verification of treatment plans in IMRT/VMAT focuses on the linear accelerator, particularly the Multi-Leaf Collimator (MLC). It involves evaluating and comparing the parameters of the treatment plans delivered by the linear accelerator with those planned. Two- or three-dimensional detector arrays and electronic portal imaging devices (EPID) have gained popularity because they are user-friendly and provide instant readouts for dose verification [3, 4]. Verification in IMRT/VMAT consisted mainly of the use of 2D measurements. However, technological advances in medical physics have led to new 3D measurement phantoms, allowing more comprehensive treatment delivery evaluation than conventional planer techniques [5].

Gamma analysis, introduced by Low et al., was used to assess results by comparing and evaluating dose distributions. This analysis relies on two fundamental concepts: dose difference and distance-to-agreement (DTA) [6, 7]. The commonly employed dosimetric criterion in studies is a 3% dose difference and 3 mm DTA, as the AAPM Task Group 119 recommends [8]. A 2% dose difference and 2 mm DTA criterion are often employed when a more stringent criterion is necessary. The gamma passing rate is used to denote the rate at which this criterion is satisfied.

The clinical significance of these criteria is not always evident. For instance, achieving a gamma passing rate of 95% in a specific treatment plan does not quantify its quality compared to another plan with a rate of 85%. Therefore, in real patient treatment scenarios, the magnitude and location of these dose errors become critically important [9].

In radiotherapy delivery, the utilization of the gamma index for PSQA may be insufficient. It is essential to have an additional method for assessing the actual dose delivered to the patient. Moreover, the gamma pass rate can vary depending on the gamma analysis type, dosimeter, Treatment Planning System (TPS), and linear accelerator setup. However, the introduction of advanced software capable of estimating the administered dose to the patient has brought about a substantial shift in PSQA practices, potentially making the gamma index method more applicable. Therefore, combining dose volume histogram (DVH) information within the patient-specific quality assurance and adding gamma passing rates is the current requirement to provide comprehensive patient-specific quality assurance [9–12].

Three-dimensional anatomy-based dose verification software combined with detector array measurements enables pre-treatment dose verification on CT images, including the calculation of DVHs. This facilitates the comparison of measured and planned patient DVHs to explore their clinical significance.

This work aims to apply DVH metrics and gamma passing rates as part of the PSQA protocol for comprehensive analysis of RapidArc treatment delivery for various anatomical sites.

Materials and methods

Study cohort

PSQA results comprising percentage gamma passing rate with different gamma criterion were analysed for the Brain (n = 15), Head and Neck (HN) (n = 30), Thorax (n = 15), and Pelvis (n = 30). The patient's cohort had varying prescription doses and fractionation

schedules, determined based on their treatment site and stage. In addition, none of the patients in our current cohort underwent stereotactic radiotherapy or radiosurgery. Furthermore, individuals with exceptional conditions, like unusual physiological circumstances or the presence of prosthetic implants, were excluded from this study.

Treatment plan preparation and delivery

Eclipse treatment planning system (TPS, version 15.6) was used to delineate the planning target volumes (PTVs) and organs at risk (OARs). Dose calculations were performed with a 6 MV flattening-filtered photon beam using two complete arcs, one in the clockwise (CW) and the other in the counterclockwise (CCW) direction. In each treatment plan, optimization was carried out using the photon optimizer (PO, version 15.6). At the same time, dose calculations were performed employing the anisotropic analytical algorithm (AAA, version 15.6) with a grid resolution of $2.5 \times 2.5 \times 2.5$ mm^3. The Millenium 120 multi-leaf collimator, integrated as a tertiary collimator in the TrueBeam linear accelerator (Varian Medical System, Palo Alto, CA), comprised 60 tungsten leaf pairs. Among these, the innermost 32 leaf pairs had a width of 5 mm each, while the outer 28 leaf pairs had a width of 10.0 mm each.

The OCTAVIUS 4D phantom (PTW, Freiburg, Germany) was used for the current study. The detector array comprises 1405 vented parallel plate ion chambers, sized at $(4.4 \times 4.4 \times 3)$ mm^3, whose centers are separated two by two by 7.07 mm. The matrix, therefore, has 27 rows of 27 chambers [11]. Before each measurement session, every 2D array was calibrated within the phantom. This was achieved by administering a 2 Gy dose at the iso-centre, using conditions equivalent to water reference conditions, via a 10×10 cm^2 field.

Software

The dose administered to the patient was determined using Verisoft (v7.2, PTW, Freiburg, Germany). The system requires input data, specifically percentage depth dose curves (PDDs), which are the basis for reconstructing 3D dose distributions within a phantom. This reconstruction begins with measurements collected from planar arrays and patient CT images. Additionally, the system depends on DICOM files to reconstruct the delivered DVH by scaling the measurements onto the patient CT set. The necessary inputs are RTStructures, RTPlan, RTDose files and phantom plan (RT plan, RT dose), which are exported from the TPS. These files are essential for facilitating the reconstruction of DVHs

Planning computed tomography as patient anatomy model for dose reconstruction

In Verisoft software, a 3D dose distribution on the CT dataset was reconstructed using the measured dose maps. In general, the human body exhibits heterogeneity in the path of the ray line, and variations in the source-to-surface distance occur due to irregular contours, as illustrated in Figure 1. It shows the schematic reconstruction of a 3D dose on a CT dataset, where the dose is reconstructed on a head and neck axial CT image. The dose measured by the current detector at the water-equivalent depth $R_{Phantom}$ corresponds to the dose of the current voxel at the water-equivalent depth R_{CT} in the CT image. Here, ρ_{Det} and ρ_{CT} represent the geometrical distances from the X-ray source focus to the current detector and voxel, respectively. The dose within the CT image along a ray line that traverses the present detector and focal point is subsequently reconstructed using the following equation [13]:

$$D_{CT} = D_{Det} \cdot \frac{TPR\left(R_{CT}\right)}{TPR\left(R_{Det}\right)} \cdot \left(\frac{\rho_{Det}}{\rho_{CT}}\right)^2$$

Gamma analysis

The present study utilised the gamma index method to evaluate the concordance between the calculated and measured dose distributions at individual points. Both global and local gamma indices were calculated, where "Global" refers to maximum dose normalization, and "local" indicates normalization concerning the corresponding position in the reference matrix. This analysis used the gamma passing rate parameter as the acceptance criterion. Agreement scores were assessed for the axial, coronal, and sagittal planes. A three-dimensional gamma analysis was conducted using the following criteria: 3mm/3%, 3mm/2%, 2mm/3%, and 2mm/2%, and a lower percentage dose threshold of 10% for global and local normalization.

Correlation analysis

In order to assess the relationship between the volumetric global and local gamma passing rates under different gamma criteria for various anatomical sites, we computed the Pearson correlation coefficient (r) along with corresponding p-values. A paired t-test was conducted, with a p-value of ≤ 0.05 considered statistically significant. r values between 0.3 and 0.49 indicate weak correlations, while moderate correlations range from 0.5 to 0.69, and strong correlations from 0.7 to 1.0.

Analysis of DVH matrices

We analyzed DVH matrices for both the clinical target volume (CTV) and planning target volume (PTV), as well as nearby OAR structures. This analysis involved comparing the Octavius measured and VeriSoft computed dose versus the planned dose values generated by the TPS for these structures. Furthermore, we assessed disparities in the minimum dose (D_{min}), maximum dose (D_{max}), and mean dose (D_{mean}) to report variations in the dose distribution within the DVHs for PTV, CTV, and OARs. Additionally, we calculated the percentage dose difference using the following formula:

$$\%D_{difference} = \frac{D_{reconstruction - ¿ D_{TPS}}}{D_{TPS}}_{¿}{}_{¿}{}_{¿}$$

Statistical analysis, including mean, standard deviation, median, and range, was conducted on the gamma passing rate using the Statistical Package for the Social Sciences (version 22; IBM Corp., Armonk, NY, USA).

Results

The mean gamma passing rate computed for each cohort was > 95% for 3%/3 mm global gamma criteria, as detailed in Table 1, which provides mean values, standard deviations, and medians within specified ranges. However, for all sites implementing 2%/3 mm and 2 mm/3% gamma criteria, the mean passing rate dropped drastically for H&N and pelvis sites by over 90% across all planes, including volume analysis.

To enhance error detection sensitivity in patient plans, we applied stringent 2%/2 mm acceptance criteria. Consequently, the volume analysis revealed that the passing rate for Brain and Head and Neck sites fell below 95%, specifically (94.69 ± 2.20) and (92.17 ± 2.53), respectively. Nonetheless, all other sites achieved passing rates exceeding 95%, except for the sagittal planes of Thorax and Pelvis, where the passing rates decreased to (94.9 ± 2.26) and (94.20 ± 3.72), respectively. Among all planes, the transverse plane consistently demonstrated the highest passing rate across all gamma criteria for every site. Introducing local gamma criteria led to a more rapid decline in passing rates than global gamma criteria. Only the 3%/3 mm and 2%/3 mm gamma criteria achieved gamma passing rates exceeding 90% for Brain,

H&N, Thorax, and Pelvis. However, in all planes and volume analyses, Brain plans managed to meet or exceed this passing rate. Notably, in local gamma analysis, the coronal plane consistently displayed the highest passing rates for Thorax and Pelvis sites compared to other planes.

A comprehensive gamma analysis, including visual representations, of all the global and local gamma criteria (3 mm/3%, 3 mm/2%, 2 mm/3%, and 2 mm/2%) for all sites. The results, accompanied by corresponding views (coronal, sagittal, and transverse) of an H&N patient, are displayed in Figure 2. Subsequently, results for other sites can be found in the Supplementary file. The data reveals that the maximum failure rate varies depending on the specific gamma criteria and cross-sectional view. Notably, a majority of the failed points are located at the field's periphery or in regions where the target and organs at risk intersect. As we tighten the gamma criteria, we observe a higher number of failed points, primarily in areas with low dose levels.

Additionally, for both global and local gamma evaluations, the 2mm/3% gamma criteria prove to be more stringent compared to the 3mm/2% criteria across all the anatomical sites mentioned. Figure 3 shows the gamma evaluation results in the patient's anatomy in different cross-sectional views for the brain, head, neck, thorax, and pelvis regions, highlighting various structures (targets and OARs). Target coverage (PTV, cyan colour), represented with red isodose line, and failed gamma points are denoted by blue and red dots in the depicted cross-sections.

The correlation between the volumetric global and local gamma passing rates was analyzed and the results are presented in Table 2. The strongest correlations were observed between the global and local gamma passing rates with a gamma criterion of 2%/3 mm and 2%/2 mm for both the H&N site (r = 0.904 with p < 0.001 and r = 0.930 with p < 0.001) and the pelvis site (r = 0.997 with p < 0.001 and r = 0.948 with p < 0.001). Moderate to strong correlations were also observed with 3%/3 mm, 2%/3 mm, and 3%/2 mm for all sites, with r values larger than 0.5 (all with p < 0.001). However, no correlations were observed for the brain and thorax sites with a gamma criterion of 2%/2 mm.

The comparison of cumulative DVH for targets and OARs for brain, head and neck, thorax, and pelvis sites is depicted in Figure 4 (A–D). It shows dose-volume variations between measured (VeriSoft) and computed doses in the TPS. Figure 5 (A–L) shows the box and whisker plots that depict the difference in maximum (D_{max}), minimum (D_{min}) and mean (D_{mean}) dose by comparing the DVH matrices from TPS and calculating the same patient in the Verisoft system. These comparisons were made for various anatomical sites, including the

brain, head and neck, thorax, and pelvis. The analysis encompassed the target areas (CTV, PTV) and the OARs specific to each site. The calculation is determined for structures located entirely inside the measuring range of the detector. No dose information from TPS is needed for anatomy-based dosimetric metrics, and the reconstruction process is also independent of γ values. The box plots for D_{min}, D_{max}, and D_{mean} in Targets and OARs revealed that the reconstruction dose performed by the detector established a better agreement with TPS-predicted ones.

The maximum deviation was observed in D_{min} for all sites. However, the maximum deviation in D_{max} was observed in H&N and Pelvis sites for targets. The dose difference in Dmean for all sites for the target was <5%, except for one patient from the H&N and Pelvis site, which is going beyond 5% in PTV. For the brain site, the percentage deviation was mainly observed in critical structures such as the optic nerves, eyes, and lens, with the maximum deviation noted in the D_{mean} values. Significant variations were seen in the head and neck sites, especially for the parotid glands and brainstem. A substantial deviation was observed in Dmin for all OARs in the thorax sites, particularly in the heart and lungs. However, the differences in D_{max} and D_{mean} doses were relatively small. The maximum variance was observed in the colon and femur heads in the pelvis site. Although the maximum dose variations in other OARs remained below 6%.

Discussion

PSQA is a standard procedure used to detect disparities between the dose calculated by a TPS system and the dose delivered by the treatment machine. In the current study, we investigated the correlation among various categories of the gamma index. Specifically, we computed both global and local gamma index concerning the maximum dose, but global gamma yielded more uniform results for all sites with an elevated passing rate. The volumetric gamma analysis assesses the entire volume, considering all planes in a time-resolved manner, similar to the approach studied by Urso et al. [14]. In addition, PSQA is indispensable for ensuring patient safety throughout advanced treatment planning and delivery, and it serves an important role to identify and mitigate errors that arise during radiotherapy treatment planning and delivery phases [15, 16].

The conventional method for pre-treatment patient-specific QA, which employs gamma passing rates, offers a means of assessing agreement, but it often lacks clinical relevance. AAPM Task Group 218, in their comprehensive examination of various aspects of PSQA, recommended a universal tolerance level for gamma pass rates, setting a minimum of 95%

for optimal clinical outcomes [17]. They proposed a gamma criterion of 3%/2 mm for a threshold dose of 10%. Additionally, a pass rate exceeding 90% is generally considered the universally accepted threshold for action.

In our present study, we evaluated the variability of the gamma passing rate across different treatment sites, employing various gamma criteria, including 3%/2 mm. Although none of our samples necessitated corrective action, some did not meet the 95% tolerance level when assessed with the 3%/2 mm criteria. Notably, most of these instances were observed in patients undergoing treatment in the H&N region. Furthermore, it was found by Lu et al. that reducing the gamma passing rate does not necessarily correlate with any immediate clinical consequences. Additionally, its accuracy is limited in regions characterized by extremely sharp dose gradients [18]. Moreover, MLC positional errors are known to be the most dominant mechanical errors affecting the RapidArc delivery. In addition, the beam complexity is not the single source contributing to the dose errors; this may arise from many measurement errors, such as a partial volume effect of ion chambers, uncertainty, dose rate ramps error, gantry sag or wobble, and neglected couch attenuation [19]. In addition, the Octavius 4D system's volumetric 3D gamma index calculates the gamma index for each voxel in the entire phantom volume, which mitigates the errors due to dose voxels. Nevertheless, adopting the strict acceptance criteria, which result in a low gamma passing rate, can be deceiving. This is because the low passing rates do not necessarily indicate significant errors in anatomical dose metrics, as many of them are false positives. Low et al. also highlighted this issue, indicating that employing 2%/2 mm criteria and a percentage gamma passing rate action level of > 90% may result in more false positives; therefore, an appropriate action level must be set [20]. In current study the H&N plans, owing to adjacent multiple target volumes due to be planned with the simultaneous integrated boost (SIB) technique, which requires a steep dose gradient between the target volumes, an overlap between the target volumes and OARs, the modulation degree of H&N Rapid Arc plans are generally much higher than that of the other treatment sites plans. Park et al. showed that the 2%/2 mm criterion is the most sensitive gamma criterion when simulated a systematic MLC error of the same magnitude. In addition, they concluded that the correlations between the global and local gamma passing rates varied according to the dosimeter type, linac type, and gamma criteria [21]. Therefore, they suggested institution-specific establishment of gamma index analysis and gamma criterion with their linac and dosimeter [22]. Furthermore, the current study found superior reliability of the volumetric local gamma with global gamma passing rates, as evidenced by the higher correlations of the local gamma passing rates across

different anatomical sites. Strong correlations were particularly notable for the H&N and pelvis sites under stringent gamma criteria (r > 0.7 with p < 0.001 for 2%/2 mm). Therefore, the strong correlation indicates that the complexity of the treatment plans varies by site, leading to a substantial reduction in gamma passing rates for both head and neck (H&N) and pelvis cases.

The implementation of DVH-based PSQA offers distinct advantages over the traditional PSQA approach. The DVH-based PSQA comprehensively assesses the dose distribution throughout the target volume and critical structures. Therefore, considering the entire DVH curve, DVH-based PSQA offers a more holistic evaluation of treatment plan quality and the dose delivered to the patient [23]. This enables the detection of potential deviations between planned and delivered doses, facilitating identifying and mitigating discrepancies. Additionally, DVH-based PSQA allows for a more patient-specific approach by accounting for individual anatomical variations and treatment objectives. Therefore, the DVH-based PSQA approach's ability to assess plan robustness makes it valuable for ensuring the safe and effective delivery of radiation therapy treatments [24].

Furthermore, Nelms et al. showed that the traditional PSQA methods do not reveal how delivery dose errors impact actual patient treatments nor offer comprehensive insights into the extent and location of dose errors within the patient [25]. In the current study, we incorporated the Octavius measurements and the patient's DICOM RT structure set, dose, and plan files to reconstruct the 3D dose within the patient and allow the computation and comparison of the DVH curves, as shown in Figure 4 (A–D), planned and delivered, for the anatomical structures that were of interest during the planning of the patient's treatment, rendering phantom-based dose analysis obsolete. Further, Figure 3 depicts the extent and location of dose errors within the patient for all anatomical sites.

According to the study by Cozzolino et al., for 2%–5% DVH Action Levels (ALs), the regions with steep dose gradients and metrics with small volumes showed relatively higher dose variations [26]. Furthermore, in a study conducted by Visser et al. concerning DVH-based head and neck IMRT QA, a stringent action level of 2.5% was applied [27]. Their investigation identified two treatment plans that required replanning. However, these plans were eventually accepted based on gamma index evaluation. In a different study, Yi, Xin et al. observed that results exceeding the DVH ALs in percentage dose differences might still be clinically acceptable [28].

In the current study, specific action limits were not defined. Nevertheless, it's worth noting that the dose delivered to the target for all treatment sites remained consistently within a 5% variation, aligning with findings in other research. Further, we have identified a significant need for modulation in cases with overlap between the target and adjacent OARs. This modulation is often necessary to meet the OAR dose constraints. Consequently, we have observed higher gamma failure points in these overlapping regions. This phenomenon is illustrated in Figures 2 and 3, where the parotid and PTV regions and the bladder and rectum regions overlap with the target region. This issue has been previously discussed by Coleman and Skourou et al., who proposed that the action levels based on DVH are overly strict [29]. Challenges arise when anatomical structures are in close proximity to the target volume, be it the PTV or CTV, including the target volume itself or OARs. Lu et al. found in their study that setting a DVH ALs of 3% was too strict for OARs near the target volume, such as the brainstem parotids within or near the PTV in the H&N plan and our study also agreed with their results for H&N sites [30].

Furthermore, Tang et al. have shown that each anatomical structure exhibits a unique sensitivity to dose errors influenced by patient geometry, fluence map complexity, target volume size, and distance from the radiation field [31]. Zhang et al.'s study aligns with these findings, highlighting that DVH-based action levels (3% or 5%) are commonly used in clinical practice [32]. However, the applicability of these levels varies among structures due to discrepancies in planning and delivery complexities.

site-specific study by Yoosuf et al. showed that more significant heterogeneity in patient geometries, such as cases involving the head and neck or the lungs, tends to lead to more pronounced disagreements [33]. Additionally, more significant discrepancies were identified in areas with steep dose gradients, suggesting that dose computation algorithms might encounter challenges when dealing with heterogeneity and penumbra regions. A similar study by Guo et al. showed that the detector reconstruction accuracy in the pelvis site was better than that in the head and neck and thorax site, in which the thorax site yielded the worst precision due to the presence of lung tissue whose mass density is close to air and less than water [34]. Therefore, they stated that the interpolation algorithm is based on the assumption that the change and development of the phenomenon are linear and uniform. In addition, better accuracy in reconstructed dose might result from more homogeneous patient structures of interest and the type of interpolation. Allgaier et al. found that DVHs generated by the TPS and Verisoft software exhibited strong concordance for treatment sites with minimal tissue inhomogeneities, like the pelvis. Conversely, larger dose disparities between

the two methods were evident for treatment sites with substantial inhomogeneity, such as the lung [35]. This is likely attributed to limitations in dose calculations within the VeriSoft DVH algorithm.

In the current study, we observed the most significant discrepancies in OAR dose differences in the Head and Neck (H&N) region. Figure 3 displays hot or cold dose voxels overlaid onto the CT images, allowing for the visualization of dose disparities like the failure points within the overlapping areas of the PTV and Parotid. Consequently, when applying more stringent criteria (2 mm/3% and 2%/2 mm), global and local gamma passing rates decreased significantly. Similar trends were observed for the pelvis region, primarily due to the large target volume. Additionally, overlapping regions between the bladder and adjacent areas contributed to these trends.

Further, the conventional gamma evaluation method considers all voxels in the dose distribution above a selected threshold, usually set at 10% or greater of the prescribed dose. However, not all voxels hold clinical significance in patient-specific QA. What indeed matters are the targets and organs at risk (OARs) as they represent the clinically relevant structures. The same was accepted by Lu et al. (18) In addition, in the current study, we have used the Octavius system with DVH, which is a stand-alone QA tool and does not rely on the dose grid computed by the TPS to ascertain measured dose distributions in a phantom or within the patient. This system assesses the patient's dose on the CT image using doses measured at corresponding points in the phantom, applying geometric and density-based corrections [36]. Typically, standalone systems are preferred for quality assurance (QA) because they are independent of TPS.

Conclusion

In addition to the DVH metric evaluation method, the gamma passing rates can compensate for the lack of dose intensity and position information of the conventional simplex gamma passing rate evaluation. DVH data directly influences clinical treatment, strengthening the correlation between patient-specific QA outcomes and clinically relevant metrics. Therefore, medical physicists should incorporate DVH-based analysis alongside gamma analysis, rather than relying solely on simplified gamma passing analysis, for a comprehensive assessment of patient-specific QA.

Authors contributions

All authors contributed to the conception or design of the work, the acquisition, analysis, or interpretation of the data. All authors were involved in drafting and commenting on the paper and have approved the final version.

Ethics approval

Ethics approval and consent to participation from Institutional Ethics Committee is "Not Applicable" due to dosimetric analysis of research work.

Consent for publication

Written consent from patients is "Not Applicable" due to dosimetric analysis of research work.

Conflict of interests

The authors declare that they have no known competing financial interests or personal relationships that could have appeared to influence the work reported in this paper.

References

1. Li J, Zhang X, Li J, et al. Impact of delivery characteristics on dose delivery accuracy of volumetric modulated arc therapy for different treatment sites. J Radiat Res. 2019; 60(5): 603–611, doi: 10.1093/jrr/rrz033, indexed in Pubmed: 31147684.

2. Chan GH, Chin LCL, Abdellatif A, et al. Survey of patient-specific quality assurance practice for IMRT and VMAT. J Appl Clin Med Phys. 2021; 22(7): 155–164, doi: 10.1002/acm2.13294, indexed in Pubmed: 34145732.

3. Bakhtiari M, Kumaraswamy L, Bailey DW, et al. Using an EPID for patient-specific VMAT quality assurance. Med Phys. 2011; 38(3): 1366–1373, doi: 10.1118/1.3552925, indexed in Pubmed: 21520847.

4. Dogan N, Mijnheer BJ, Padgett K, et al. AAPM Task Group Report 307: Use of EPIDs for Patient-Specific IMRT and VMAT QA. Med Phys. 2023; 50(8): e865–e903, doi: 10.1002/mp.16536, indexed in Pubmed: 37384416.

5. Manna S. Evaluation of Patient-Specific Quality Assurance for RapidArc Treatment Delivery Using Dose Volume Histogram. J Polymer Compos. 2023, doi: 10.37591/jopc.v11i07.126106.

6. Low DA, Harms WB, Mutic S, et al. A technique for the quantitative evaluation of dose distributions. Med Phys. 1998; 25(5): 656–661, doi: 10.1118/1.598248, indexed in Pubmed: 9608475.

7. Low DA, Moran JM, Dempsey JF, et al. Dosimetry tools and techniques for IMRT. Med Phys. 2011; 38(3): 1313–1338, doi: 10.1118/1.3514120, indexed in Pubmed: 21520843.

8. Ezzell GA, Burmeister JW, Dogan N, et al. IMRT commissioning: multiple institution planning and dosimetry comparisons, a report from AAPM Task Group 119. Med Phys. 2009; 36(11): 5359–5373, doi: 10.1118/1.3238104, indexed in Pubmed: 19994544.

9. Song JHo, Shin HJ, Kay CS, et al. Dosimetric verification by using the ArcCHECK system and 3DVH software for various target sizes. PLoS One. 2015; 10(3): e0119937, doi: 10.1371/journal.pone.0119937, indexed in Pubmed: 25807544.

10. Vikraman S, Manigandan D, Karrthick KP, et al. Quantitative evaluation of 3D dosimetry for stereotactic volumetric-modulated arc delivery using COMPASS. J Appl Clin Med Phys. 2014; 16(1): 5128, doi: 10.1120/jacmp.v16i1.5128, indexed in Pubmed: 25679152.

11. Stelljes TS, Harmeyer A, Reuter J, et al. Dosimetric characteristics of the novel 2D ionization chamber array OCTAVIUS Detector 1500. Med Phys. 2015; 42(4): 1528–1537, doi: 10.1118/1.4914151, indexed in Pubmed: 25832043.

12. Stasi M, Bresciani S, Miranti A, et al. Pretreatment patient-specific IMRT quality assurance: a correlation study between gamma index and patient clinical dose volume histogram. Med Phys. 2012; 39(12): 7626–7634, doi: 10.1118/1.4767763, indexed in Pubmed: 23231310.

13. Thomas SJ. Relative electron density calibration of CT scanners for radiotherapy treatment planning. Br J Radiol. 1999; 72(860): 781–786, doi: 10.1259/bjr.72.860.10624344, indexed in Pubmed: 10624344.

14. Urso P, Lorusso R, Marzoli L, et al. Practical application of Octavius -4D: Characteristics and criticalities for IMRT and VMAT verification. J Appl Clin Med Phys. 2018; 19(5): 517–524, doi: 10.1002/acm2.12412, indexed in Pubmed: 30009564.

15. Lehmann J, Hussein M, Barry MA, et al. SEAFARER — A new concept for validating radiotherapy patient specific QA for clinical trials and clinical practice. Radiother Oncol. 2022; 171: 121–128, doi: 10.1016/j.radonc.2022.04.019, indexed in Pubmed: 35461949.

16. Das S, Kharade V, Pandey VP, et al. Gamma Index Analysis as a Patient-Specific Quality Assurance Tool for High-Precision Radiotherapy: A Clinical Perspective of Single Institute Experience. Cureus. 2022; 14(10): e30885, doi: 10.7759/cureus.30885, indexed in Pubmed: 36337776.

17. Miften M, Olch A, Mihailidis D, et al. Tolerance limits and methodologies for IMRT measurement-based verification QA: Recommendations of AAPM Task Group No. 218. Med Phys. 2018; 45(4): e53–e83, doi: 10.1002/mp.12810, indexed in Pubmed: 29443390.

18. Lu W, Li Y, Huang W, et al. Optimizing the Region for Evaluation of Global Gamma Analysis for Nasopharyngeal Cancer (NPC) Pretreatment IMRT QA by COMPASS: A Retrospective Study. Front Oncol. 2022; 12: 859415, doi: 10.3389/fonc.2022.859415, indexed in Pubmed: 35774127.

19. Du W, Cho SH, Zhang X, et al. Quantification of beam complexity in intensity-modulated radiation therapy treatment plans. Med Phys. 2014; 41(2): 021716, doi: 10.1118/1.4861821, indexed in Pubmed: 24506607.

20. Low C, Toye W, Phung P, et al. Patient-Specific Quality Assurance Protocol for Volumetric Modulated Arc Therapy using Dose Volume Histogram. J Med Phys. 2018; 43(2): 112–118, doi: 10.4103/jmp.JMP_138_17, indexed in Pubmed: 29962689.

21. Park JM, Kim JI, Park SY, et al. Reliability of the gamma index analysis as a verification method of volumetric modulated arc therapy plans. Radiat Oncol. 2018; 13(1): 175, doi: 10.1186/s13014-018-1123-x, indexed in Pubmed: 30217163.

22. Rajasekaran D, Jeevanandam P, Sukumar P, et al. A study on the correlation between plan complexity and gamma index analysis in patient specific quality assurance of

volumetric modulated arc therapy. Rep Pract Oncol Radiother. 2015; 20(1): 57–65, doi: 10.1016/j.rpor.2014.08.006, indexed in Pubmed: 25535586.

23. Gong C, Zhu K, Lin C, et al. Efficient dose-volume histogram-based pretreatment patient-specific quality assurance methodology with combined deep learning and machine learning models for volumetric modulated arc radiotherapy. Med Phys. 2022; 49(12): 7779–7790, doi: 10.1002/mp.16010, indexed in Pubmed: 36190117.

24. Chen L, Luo H, Li S, et al. Pretreatment patient-specific quality assurance prediction based on 1D complexity metrics and 3D planning dose: classification, gamma passing rates, and DVH metrics. Radiat Oncol. 2023; 18(1): 192, doi: 10.1186/s13014-023-02376-4, indexed in Pubmed: 37986008.

25. Nelms B, Stambaugh C, Hunt D, et al. Methods, software and datasets to verify DVH calculations against analytical values: Twenty years late(r). Med Phys. 2015; 42(8): 4435–4448, doi: 10.1118/1.4923175, indexed in Pubmed: 26233174.

26. Cozzolino M, Oliviero C, Califano G, et al. Clinically relevant quality assurance (QA) for prostate RapidArc plans: gamma maps and DVH-based evaluation. Phys Med. 2014; 30(4): 462–472, doi: 10.1016/j.ejmp.2014.01.003, indexed in Pubmed: 24480527.

27. Visser R, Wauben DJL, de Groot M, et al. Evaluation of DVH-based treatment plan verification in addition to gamma passing rates for head and neck IMRT. Radiother Oncol. 2014; 112(3): 389–395, doi: 10.1016/j.radonc.2014.08.002, indexed in Pubmed: 25154319.

28. Yi X, Lu WL, Dang J, et al. A comprehensive and clinical-oriented evaluation criteria based on DVH information and gamma passing rates analysis for IMRT plan 3D verification. J Appl Clin Med Phys. 2020; 21(8): 47–55, doi: 10.1002/acm2.12910, indexed in Pubmed: 32436351.

29. Coleman L, Skourou C. Sensitivity of volumetric modulated arc therapy patient specific QA results to multileaf collimator errors and correlation to dose volume histogram based metrics. Med Phys. 2013; 40(11): 111715, doi: 10.1118/1.4824433, indexed in Pubmed: 24320423.

30. Racka I, Majewska K, Winiecki J. Three-dimensional conformal radiotherapy (3D-CRT) vs. volumetric modulated arc therapy (VMAT) in deep inspiration breath-hold (DIBH) technique in left-sided breast cancer patients-comparative analysis of dose distribution and estimation of projected secondary cancer risk. Strahlenther Onkol.

2023; 199(1): 90–101, doi: [10.1007/s00066-022-01979-2](#), indexed in
Pubmed: [35943553](#).

31. Tang Du, Yang Z, Dai X, et al. Evaluation of Delta Anatomy in 3D Patient-Specific
    IMRT Quality Assurance. Technol Cancer Res Treat. 2020; 19: 1533033820945816,
    doi: [10.1177/1533033820945816](#), indexed in Pubmed: [32720589](#).

32. Zhang H, Lu W, Cui H, et al. Assessment of Statistical Process Control Based DVH
    Action Levels for Systematic Multi-Leaf Collimator Errors in Cervical Cancer
    RapidArc Plans. Front Oncol. 2022; 12: 862635, doi: [10.3389/fonc.2022.862635](#),
    indexed in Pubmed: [35664736](#).

33. Mohamed Yoosuf AB, AlShehri S, Alhadab A, et al. DVH analysis using a
    transmission detector and model-based dose verification system as a comprehensive
    pretreatment QA tool for VMAT plans: Clinical experience and results. J Appl Clin
    Med Phys. 2019; 20(11): 80–87, doi: [10.1002/acm2.12743](#), indexed in
    Pubmed: [31605456](#).

34. Guo Y, Hu J, Li Y, et al. Correlation between patient-specific quality assurance in
    volumetric modulated arc therapy and 2D dose image features. Sci Rep. 2023; 13(1):
    4051, doi: [10.1038/s41598-023-30719-4](#), indexed in Pubmed: [36899027](#).

35. RP S. Gamma Evaluation with Octavius 4D Phantom for PreTreatment of Modern
    Radiotherapy Treatment Techniques. Int J Nucl Med Radioact Subst. 2019; 2(2),
    doi: [10.23880/ijnmrs-16000117](#).

36. Sadagopan R, Bencomo JA, Martin RL, et al. Characterization and clinical evaluation
    of a novel IMRT quality assurance system. J Appl Clin Med Phys. 2009; 10(2): 104–
    119, doi: [10.1120/jacmp.v10i2.2928](#), indexed in Pubmed: [19458595](#).

Table 1. This presents the gamma passing rates for the brain, head and neck, thorax, and
pelvis sites. The passing rates are provided as both the mean and standard deviation (on the
left side) and the median with a range (on the right side) for 3D (coronal, sagittal, and
transverse planes) and volumetric gamma indices (local and global)

	Site	Gamma Criteria	Coronal	Sagittal	Transverse	Volume Analysis	Coronal	Sagittal	Transverse	Volume Analysis

			Mean ± SD				Median (Range)			
3D–Global Gamma	**Brain (n = 15)**	3%/3 mm	99.46 ± 0.52	99.58 ± 0.50	99.56 ± 0.50	99.29 ± 0.57	99.8 (98.4–100)	99.8 (98.2–100)	99.8 (98.4–100)	99.5 (98.0–99.9)
		2%/3 mm	98.48 ± 1.06	98.99 ± 0.89	98.83 ± 1.09	98.45 ± 1.01	98.8 (96.5–99.8)	99.4 (96.9–100)	99.1 (96.3–100)	98.7 (96.2–99.7)
		3%/2 mm	97.51 ± 1.78	97.68 ± 1.45	97.86 ± 1.81	97.46 ± 1.54	97.9 (94.3–99.9)	97.6 (94.1–99.9)	98.0 (92.9–100)	97.5 (94.5–99.7)
		2%/2 mm	94.88 ± 2.75	95.53 ± 2.15	95.53 ± 3.23	94.69 ± 2.20	95.4 (89.5–98.4)	95.4 (91.5–99.2)	95.2 (86.9–99.6)	94.7 (90.5–98.2)
	Head and Neck (n = 30)	3%/3 mm	99.14 ± 0.53	99.01 ± 0.54	99.47 ± 0.79	98.71 ± 0.43	99.5 (97.9–99.9)	99.6 (97.2–99.8)	99.9 (96.75–100)	99.2 (97.82–99.95)
		2%/3 mm	97.53 ± 1.35	96.97 ± 1.37	98.70 ± 1.54	96.85 ± 1.75	97.6 (95.62–99.6)	97.4 (92.5–99.3)	99.4 (93.5–99.9)	97.2 (93.20–99.50)
		3%/2 mm	96.75 ± 1.65	97.23 ± 1.53	98.47 ± 1.67	96.87 ± 1.56	97.5 (94.5–98.9)	97.8 (93.2–98.9)	99.1 (91.8–99.8)	97.5 (93.20–99.5)
		2%/2 mm	93.15 ± 2.83	92.35 ± 3.27	95.35 ± 3.05	92.17 ± 2.53	92.8 (87.8–98.7)	93.7 (83.5–96.68)	96.2 (84.2–99.6)	92.32 (85.1–97.8)

Region	Criterion								
Thorax (n = 15)	3%/3 mm	99.5 ± 0.43	99.6 ± 0.27	99.8 ± 0.21	99.4 ± 0.30	99.7 (98.3–99.9)	99.7 (99.1–100.0)	99.9 (99.3–100.0)	99.5 (98.9–99.9)
	2%/3 mm	98.5 ± 0.74	98.3 ± 0.95	98.9 ± 0.99	97.8 ± 0.74	98.6 (97.3–99.7)	98.7 (96.2–99.4)	99.3 (96.3–99.9)	97.9 (96.5–99.1)
	3%/2 mm	98.4 ± 1.04	98.3 ± 0.97	99.0 ± 0.72	98.4 ± 0.66	98.9 (96.1–99.5)	98.1 (97.1–99.9)	99.2 (97.3–99.9)	98.3 (97.3–99.5)
	2%/2 mm	96.6 ± 1.34	94.9 ± 2.26	96.5 ± 2.39	95 ± 1.64	96.8 (94.3–98.6)	95.4 (90.5–98.0)	96.8 (90.9–99.6)	94.5 (92.7–98.0)
Pelvis (n = 30)	3%/3 mm	99.72 ± 0.38	99.52 ± 0.62	99.9 ± 0.37	99.75 ± 0.39	99.7 (98.3–100)	99.3 (97.2–99.9)	99.8 (98.2–100)	99.8 (98.60–100)
	2%/3 mm	98.51 ± 0.96	97.47 ± 2.43	98.74 ± 1.43	98.27 ± 1.51	98.6 (95.8–99.9)	98.0 (89.2–99.6)	98.7 (92.1–99.9)	98.9 (94.20–99.80)
	3%/2 mm	98.92 ± 0.91	98.15 ± 1.41	99.13 ± 0.92	98.81 ± 0.96	99.0 (95.7–99.7)	98.15 (95.7–99.8)	99.1 (95.3–100)	99.6 (96.90–99.80)
	2%/2 mm	95.98 ± 2.15	94.20 ± 3.72	95.78 ± 3.15	95.75 ± 2.91	95.8 (91.1–98.9)	94.1 (82.1–98.2)	96.7 (85.2–99.6)	96.37 (87.20–98.90)

	Site	Gamma criteria	Coronal	Sagittal	Transverse	Volume analysis	Coronal	Sagittal	Transverse	Volume analysis
			Mean ± SD				Median (Range)			
3D-Local Gamma	Brain (n = 15)	3%/3 mm	97.88 ± 1.79	98.66 ± 0.94	97.73 ± 1.91	97.11 ± 1.661	98.6 (93.7–99.9)	98.5 (97.4–100)	98.3 (93.7–99.7)	96.8 (94.5–99.4)
		2%/3 mm	96.70 ± 2.24	97.99 ± 1.33	96.88 ± 2.36	96.11 ± 1.88	97.6 (91.8–99.2)	97.6 (96.0–100)	97.3 (91.9–99.4)	95.6 (93.1–98.9)
		3%/2 mm	92.81 ± 4.53	94.32 ± 2.32	92.42 ± 5.07	90.74 ± 3.64	94.7 (85.0–98.1)	94.5 (90.6–99.2)	94.0 (80.8–98.5)	90.5 (85.0–96.7)
		2%/2 mm	88.06 ± 5.23	92.33 ± 2.90	88.42 ± 6.62	87.17 ± 4.04	89 (80.6–96.5)	92.4 (88.2–97.6)	88.7 (76.4–96.5)	87.4 (81.8–93.9)
	Head and Neck (n = 30)	3%/3 mm	95.20 ± 1.75	93.75 ± 2.62	95.35 ± 2.51	92.15 ± 2.83	95.3 (90.7–98.3)	94.5 (84.7–97.8)	96.7 (87.3–99.8)	92.1 (84.6–97.4)
		2%/3 mm	93.15 ± 2.51	91.2 ± 3.15	94.25 ± 3.27	90.25 ± 3.33	93.7 (87.7–97.8)	92.6 (81.5–96.6)	95.0 (83.7–99.8)	90.6 (81.2–96.5)
		3%/2 mm	86.71 ± 3.69	84.12 ± 4.17	87.78 ± 4.14	80.94 ± 4.92	86.8 (78.8–93.5)	85.1 (69.8–91.5)	88.5 (72.1–98.7)	81.6 (70.2–90.8)
		2%/2 mm	81.47 ± 4.58	80.39 ± 5.13	83.43 ± 5.34	76.14 ± 5.18	82.3 (73.9–90.7)	80.8 (65.5–88.2)	83.8 (66.4–97.2)	77.4 (63.1–87.5)
	Thor	3%/3 mm	98.5 ± 0.74	98.3 ± 0.95	98.9 ± 0.99	97.8 ± 0.74	99.2 (98.2–99.8)	97.0 (95.3–99.3)	98.3 (93.3–99.8)	95.4 (94.0–96.5)
		2%/3 mm	98.2 ± 0.92	95.3 ± 1.40	96.1 ± 2.03	93.5 ± 1.00	98.0 (96.8–)	95.8 (92.8–)	96.8 (90.7–98)	93.4 (92.1–)
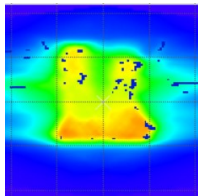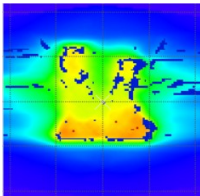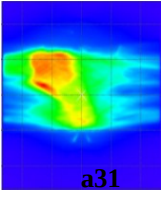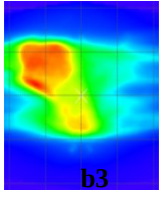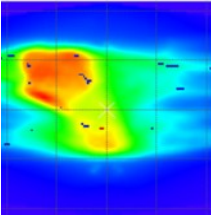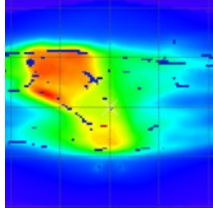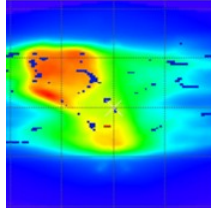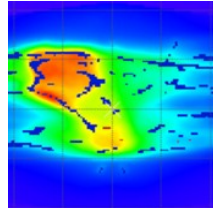
SD — standard deviation

Table 2. Shows the **c**orrelations between the global and local gamma passing rates for different gamma criterion and anatomical sites

Sites	Ga mma criteria	r	p
Brain	3%/3 mm	0.628	0.016
	2%/3 mm	0.770	0.001
	3%/2 mm	0.790	0.001
	2%/2 mm	0.348	0.223
Head and Neck	3%/3 mm	0.809	0.000
	2%/3 mm	0.904	0.000
	3%/2 mm	0.853	0.000
	2%/2 mm	0.930	0.000
Thorax	3%/3 mm	0.674	0.008
	2%/3 mm	0.732	0.003
	3%/2 mm	0.587	0.027
	2%/2 mm	0.491	0.068
Pelvis	3%/3 mm	0.850	0.000
	2%/3 mm	0.997	0.000
	3%/2 mm	0.884	0.000
	2%/2 mm	0.948	0.000
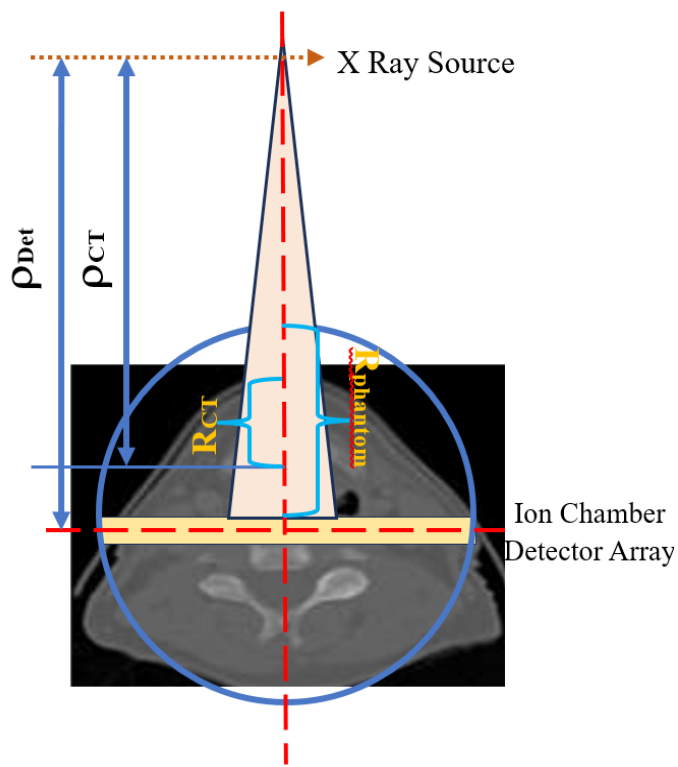
Figure 1. The schematic reconstruction of a 3D dose on a computed tomography (CT) dataset, where the dose is reconstructed on an axial CT image of the head and neck

Global Gamma Criteria (DD/DTA)	3%/3mm	2mm/3%	3mm/2%	2mm/2%
Coronal	99.1	96.4	97.4	91.4
a1 b1				
Transverse	99.9	99.2	99.6	99.1
a2 b2				
Sagittal	99.3	96.6	97.2	91.1
a31 b3				

Figure 2. The gamma evaluation of head and neck (H&N) site, comparing the measured dose maps (b1, b2, and b3) with the calculated dose maps (a1, a2, and a3) using different global gamma criteria, DD/DTA (3%/3 mm, 2%/3 mm, 3%/2 mm, and 2%/2 mm). The evolution shows the variation in gamma passing percentages across various planes (coronal, transverse, and sagittal). In the evaluation maps, blue and red dots represent failed gamma points with values < 0.95 and > 1, respectively

	Axial	Coronal	Sagittal
Brain			
Head and Neck			
Thorax			
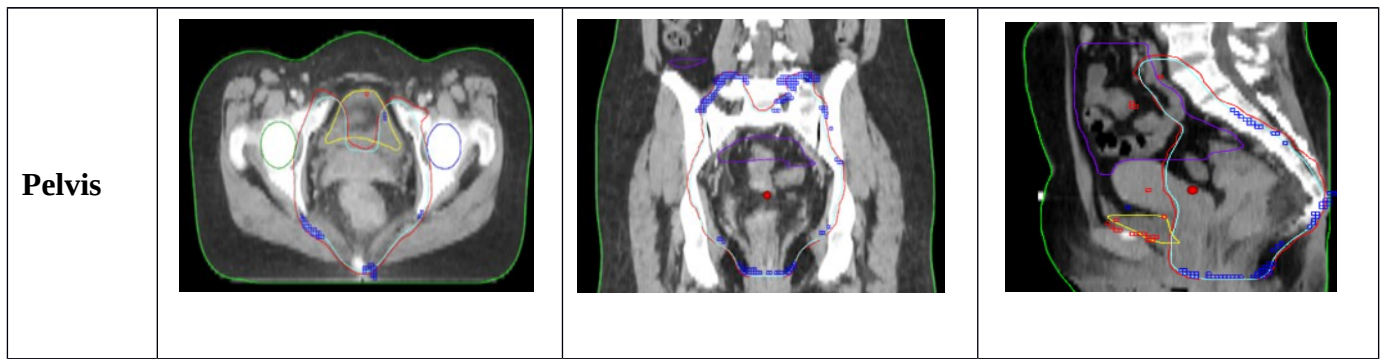
Figure 3. Cross-sections of the brain, head, neck, thorax, and pelvis regions, highlighting various structures [targets and organs at risk (OARs)]. Target coverage [planning target volume (PTV), cyan colour[is represented by the red isodose line, and failed gamma points are denoted by blue and red dots in the depicted cross-sections. The potential benefit of dose volume histogram (DVH), in contrast to other methods, was its capacity to display hot or cold dose voxels overlaid onto the CT images, allowing for the visualization of dose disparities relative to patient anatomy.
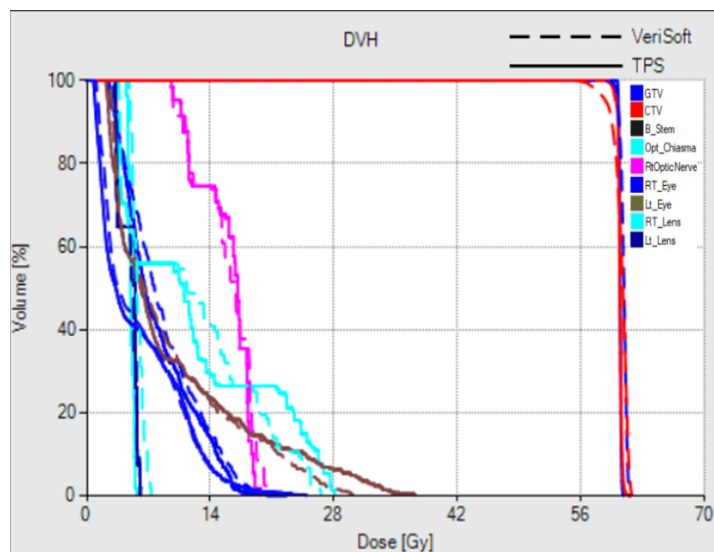
(a) Brain
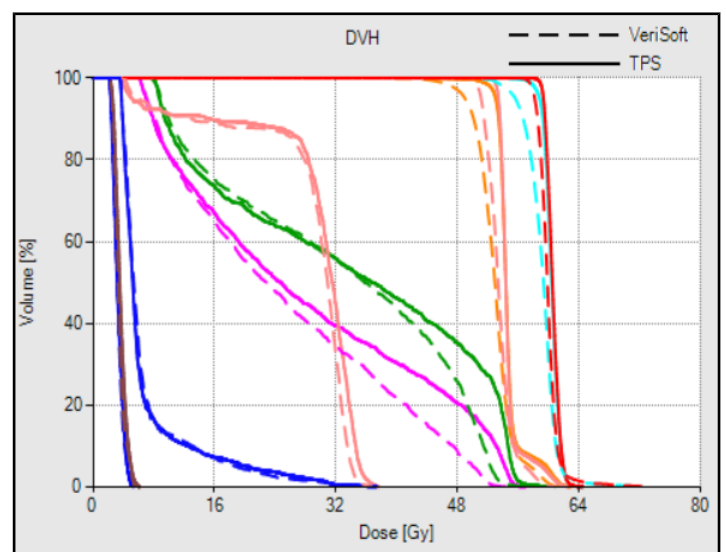
(b) Head and Neck
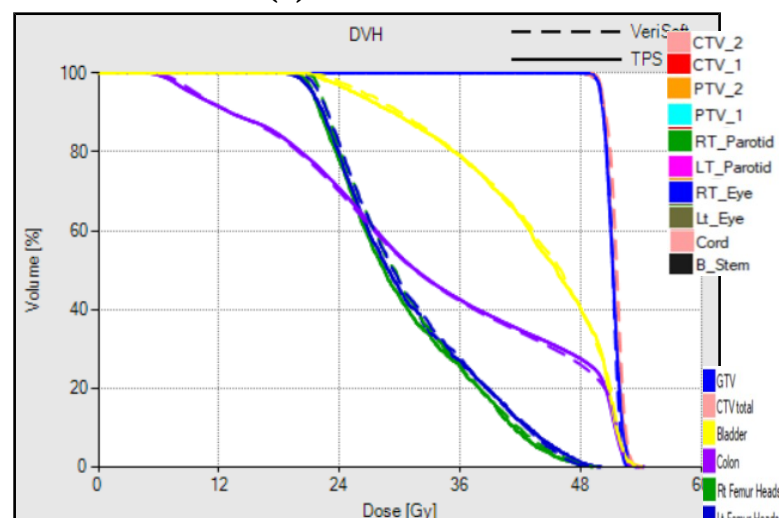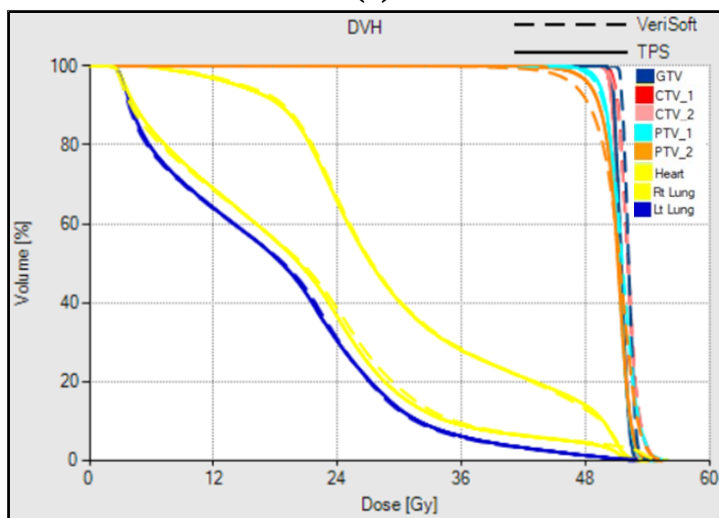
(c) **Thorax**   (d) **Pelvis**

Figure 4 A–D. The cumulative dose-volume histogram (DVH) for targets and organs at risk (OARs) in the brain, head and neck, thorax, and pelvis. It compares dose-volume variations between measured (VeriSoft) and computed doses in the treatment planning system (TPS)

Fig. 5a

Fig.5b

Fig.5c

Dmean

Dose difference for Target and OARs of Brain Group (n=15)

Fig.5d

Dmin

Dose difference for Target and OARs of HN Group (n=30)

Fig.5e

Dmax

Dose difference for Target and OARs of HN Group (n=30)

Fig.5f

Fig.5g

Dmin

Dose difference for Target and OARs of Thorax Group (n=15)

Fig.5h

Dmax

Dose difference for Target and OARs of Thorax Group (n=15)

Fig.5i

Dmean

Dose difference for Target and OARs of Thorax Group (n=15)
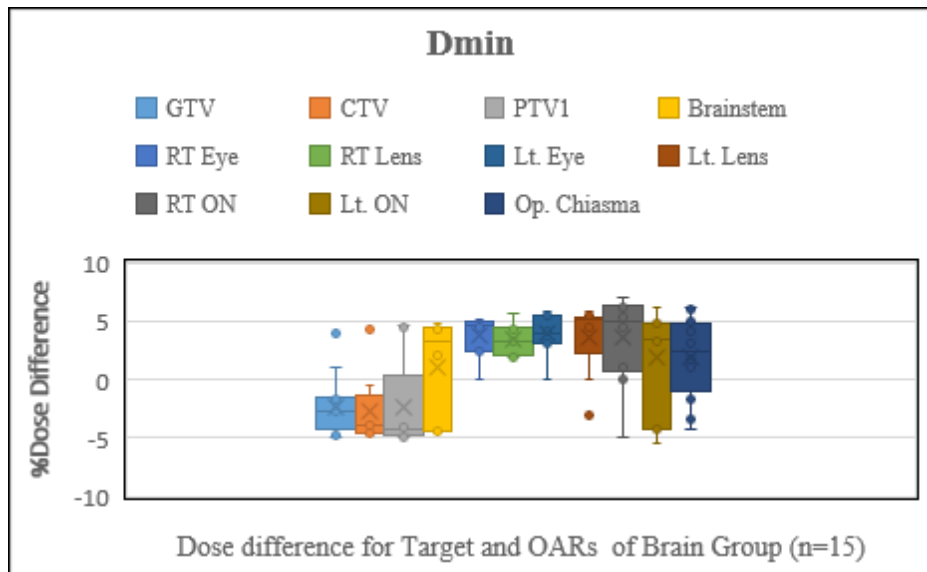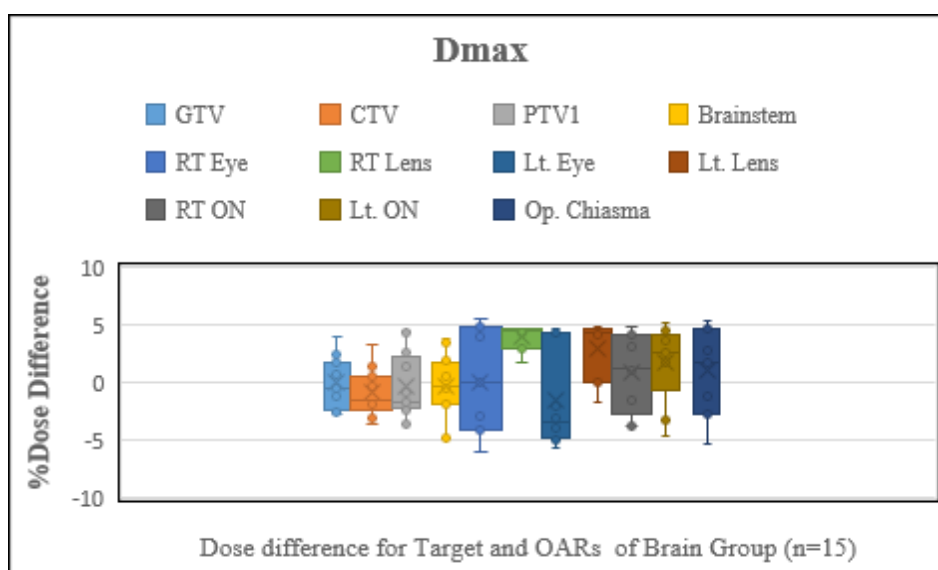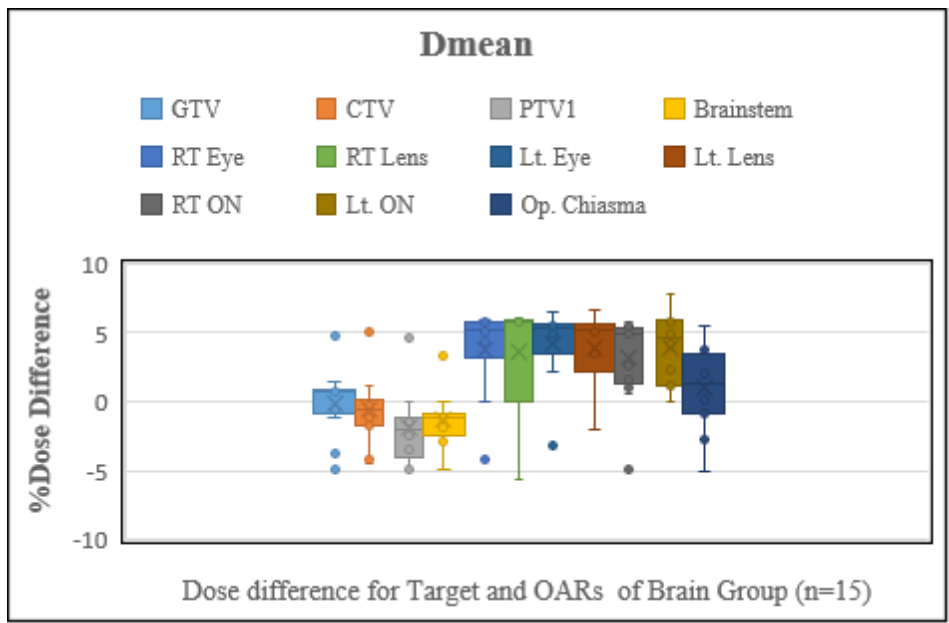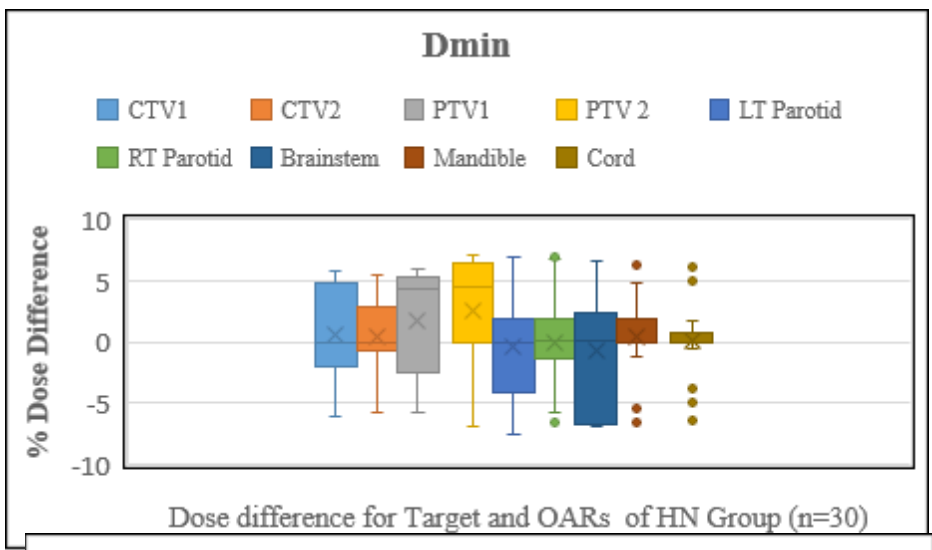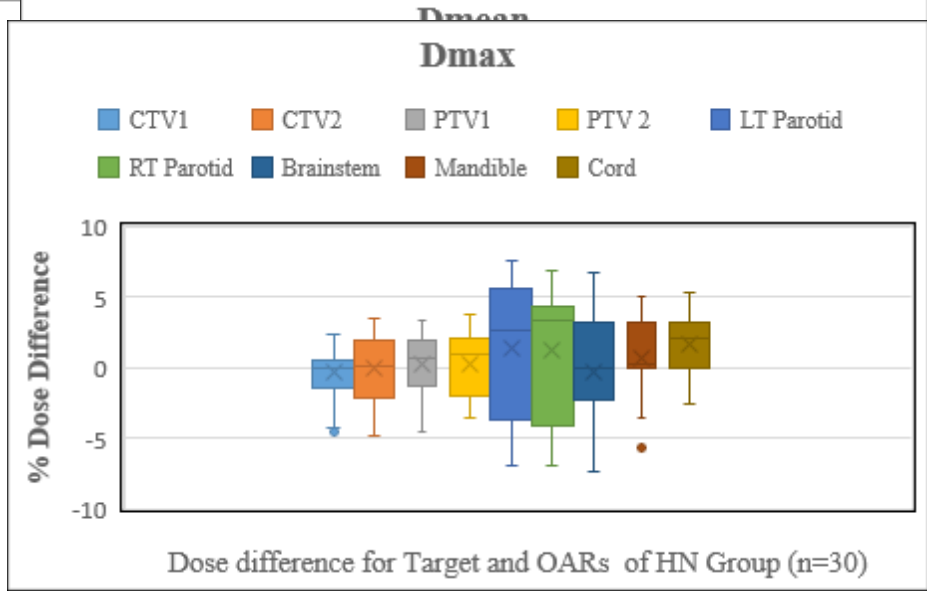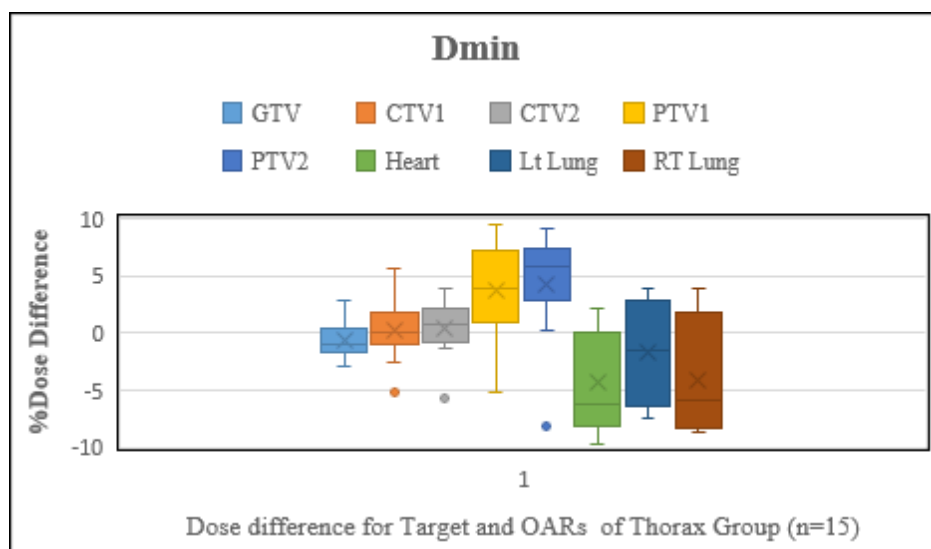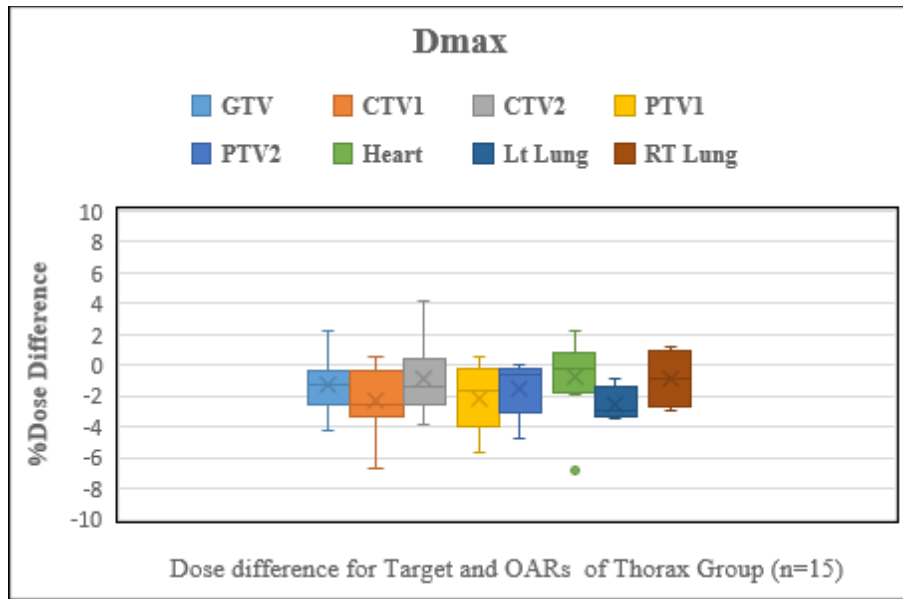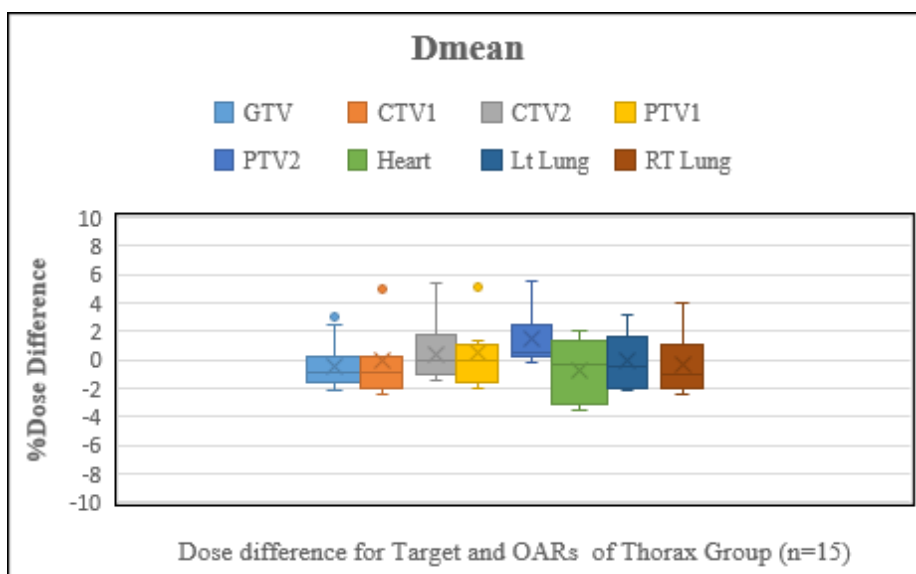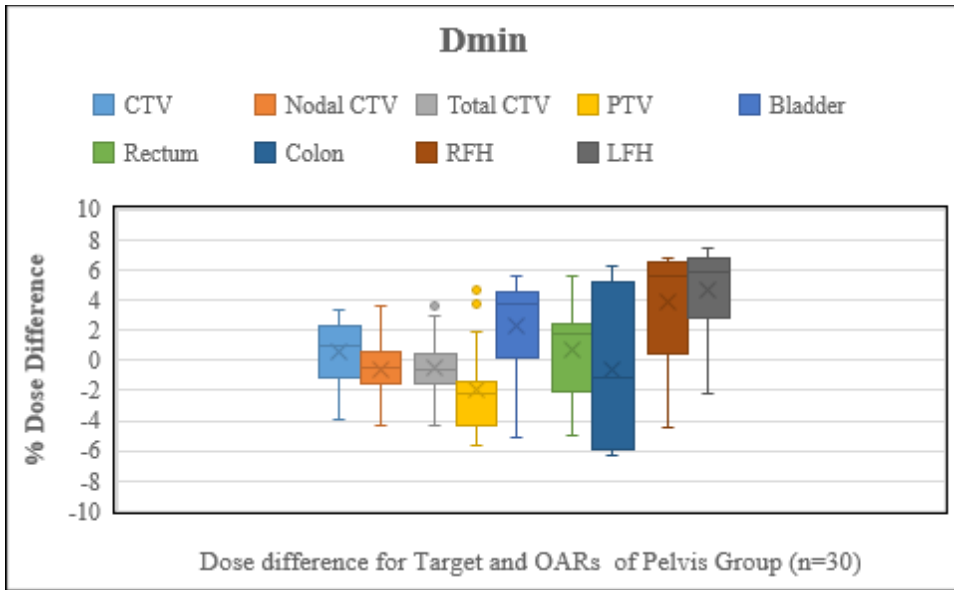
Fig. 5j
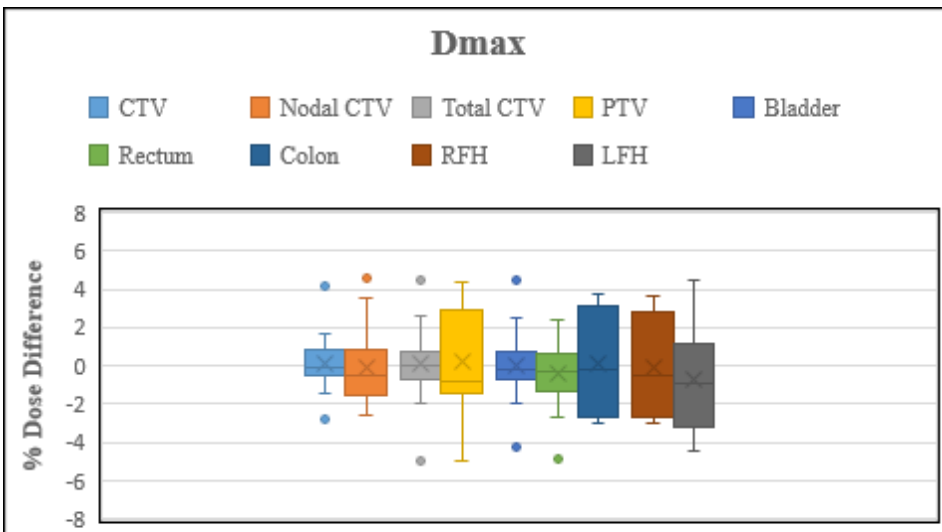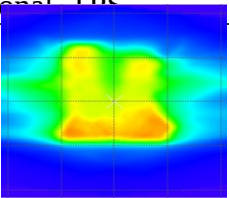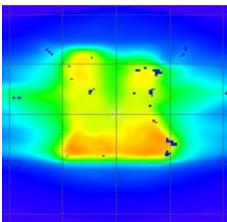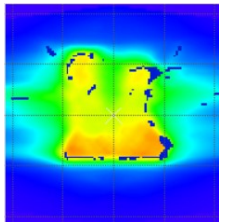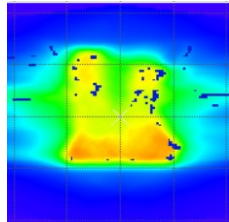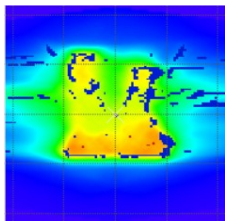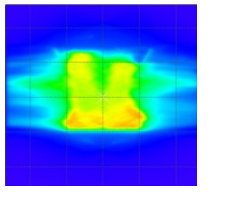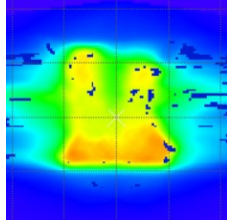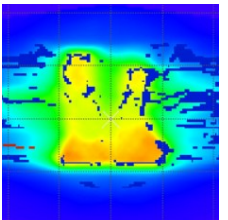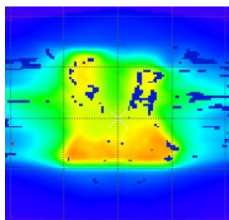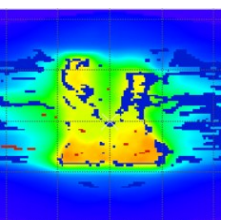
Fig.5k
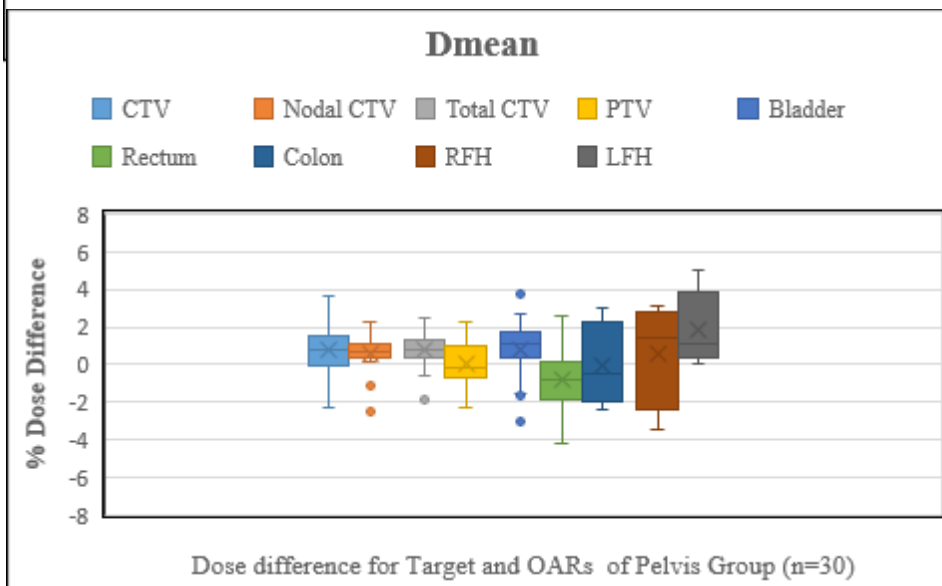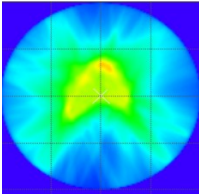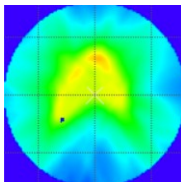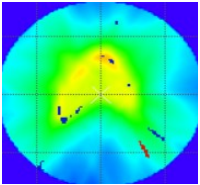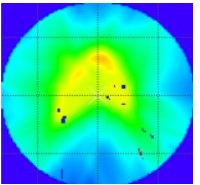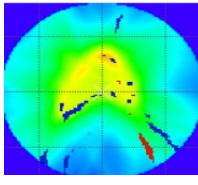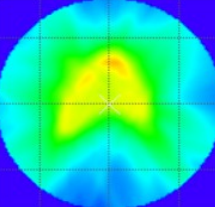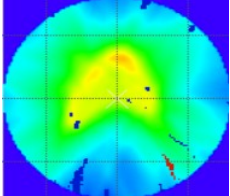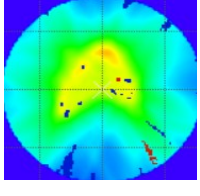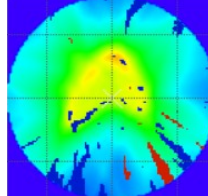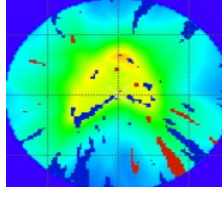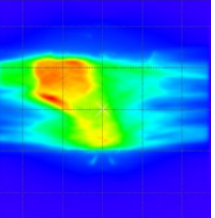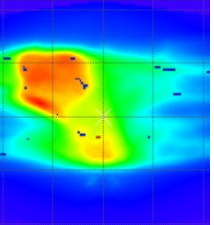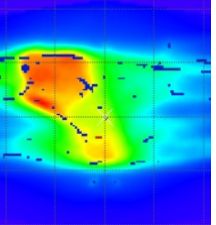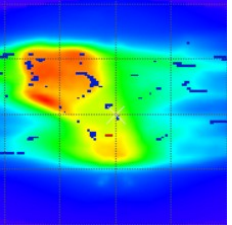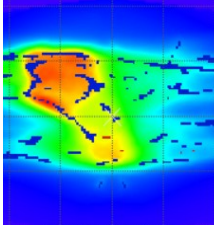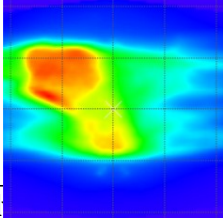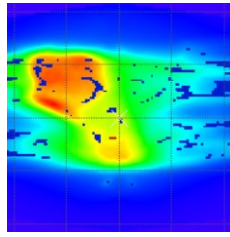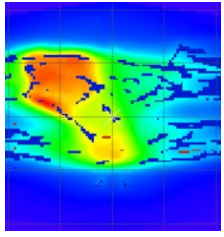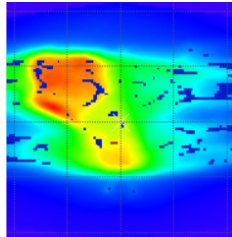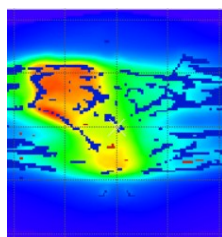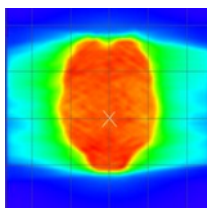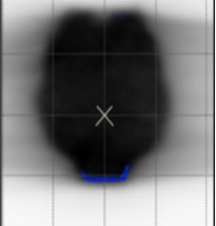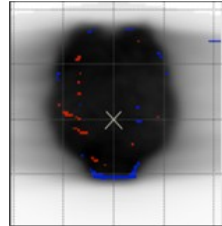
Fig.5l
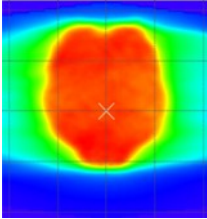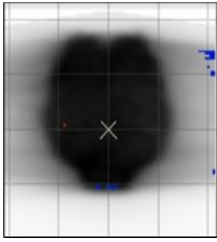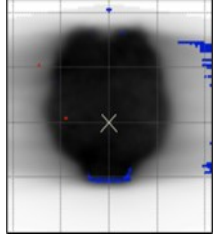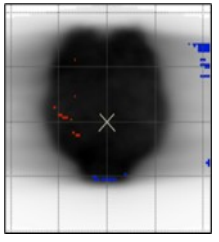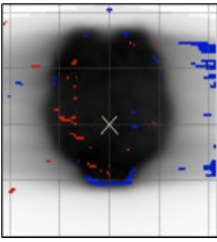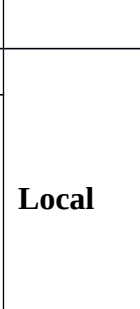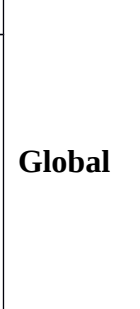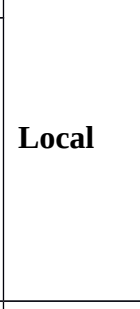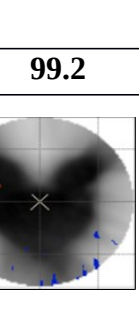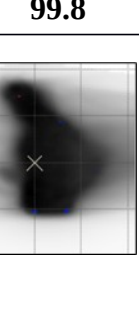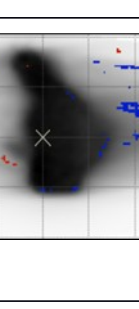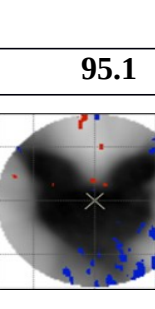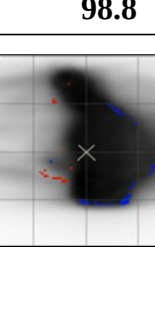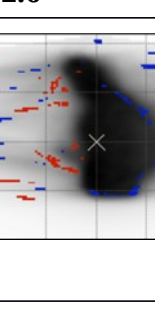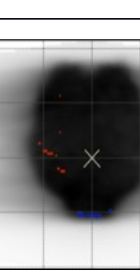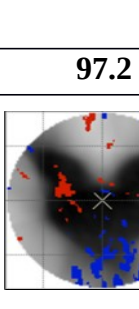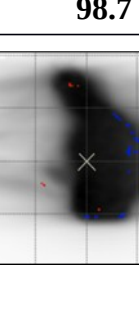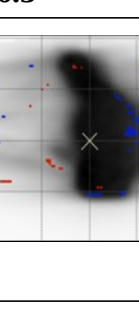
Figure 5 A–L. The box and whisker plots that depict the percentage difference between the measured (VeriSoft) and computed dose (Treatment Planning System, TPS). These comparisons were made for various anatomical sites that includes brain, head and neck, thorax, and pelvis. The analysis encompassed both the target areas [clinical target volume (CTV), planning target volume (PTV)] and the organs at risk (OARs) specific to each site
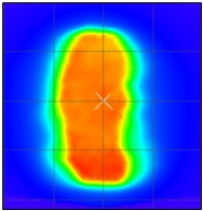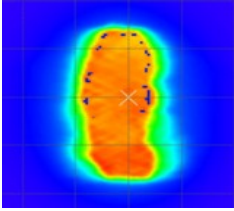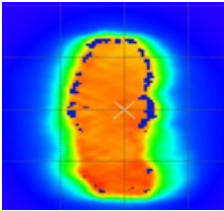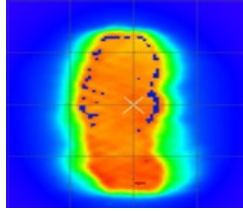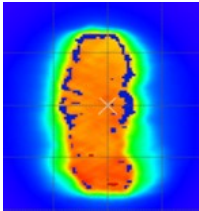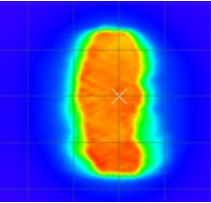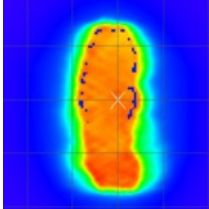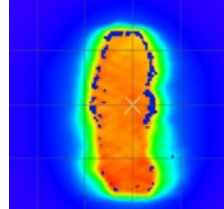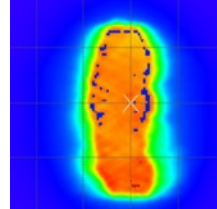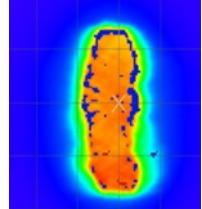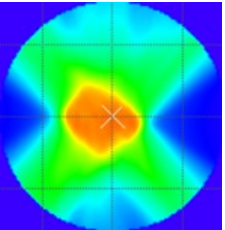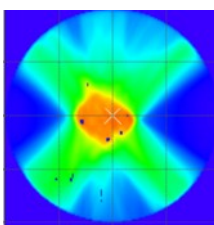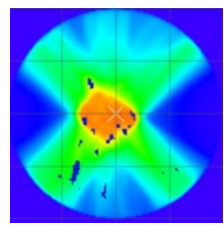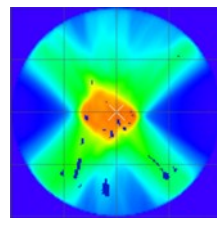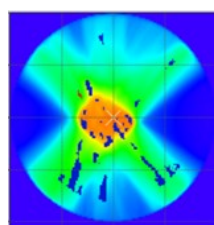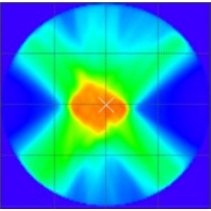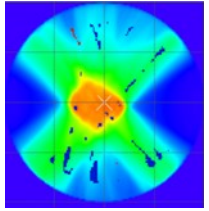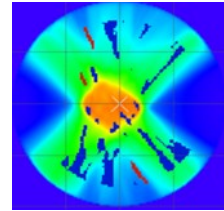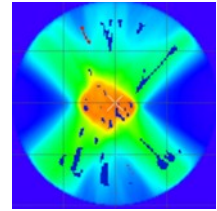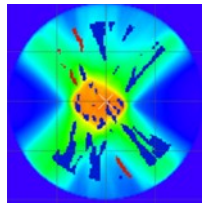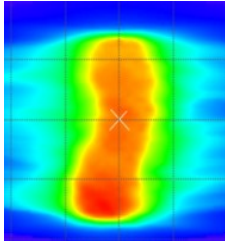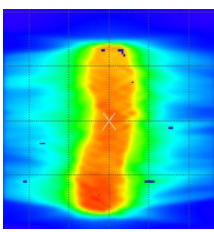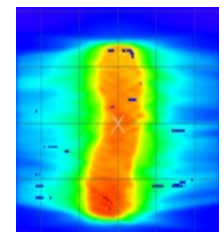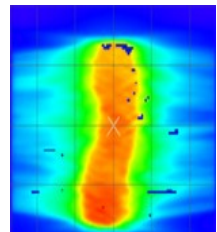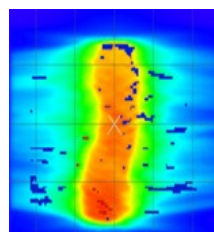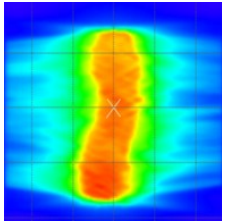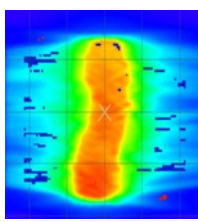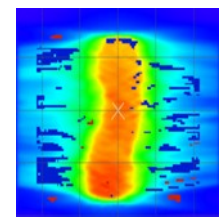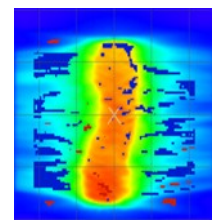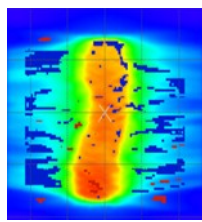
Supplemetary File
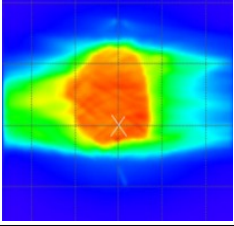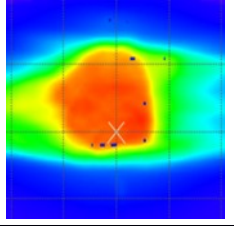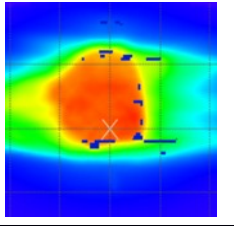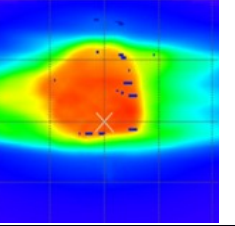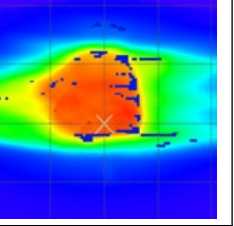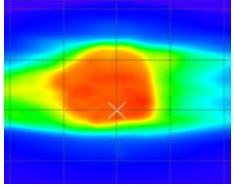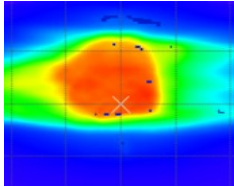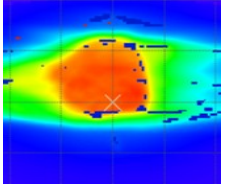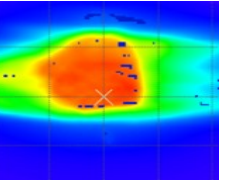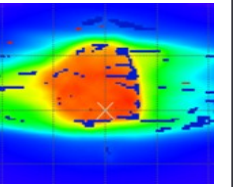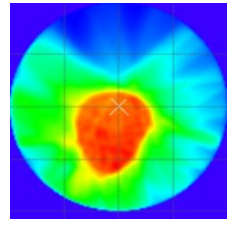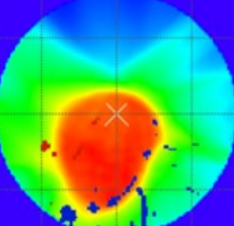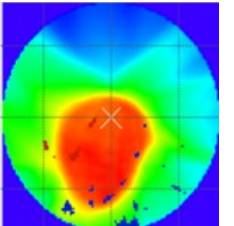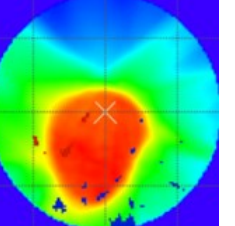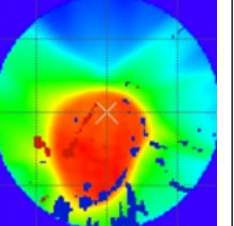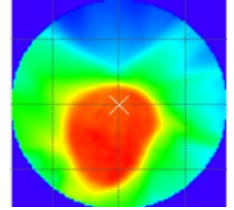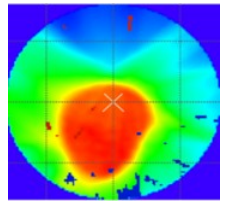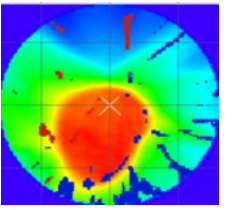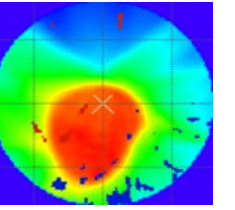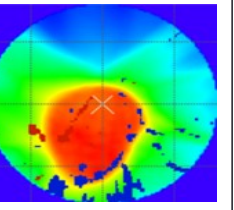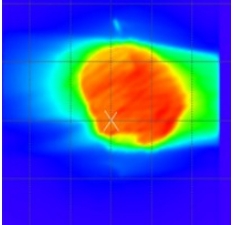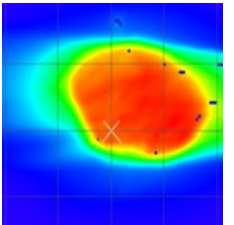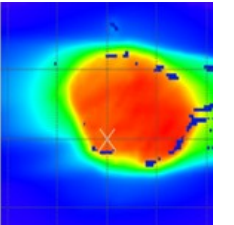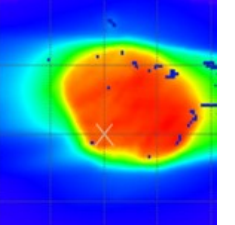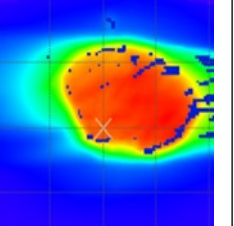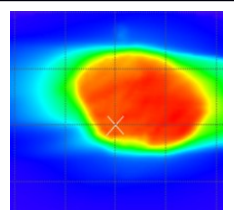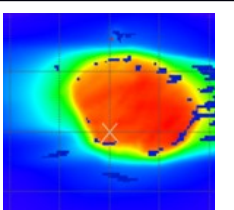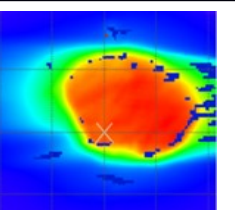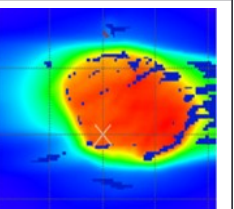
Head and Neck	Gamma	3%/3mm	2mm/3%	3mm/2%	2mm/2%
Coronal_TPS	Global	99.1	96.4	97.4	91.4
Coronal_Cal	Local	94.6	83.2	92.5	78.3
Transverse_TPS	Global	99.9	99.2	99.6	99.1

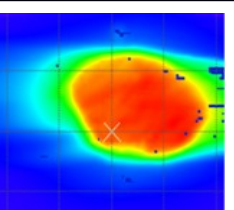|					
Transverse_Cal		**98.2**	**97.5**	**92.0**	**89.4**
	Local				
Saggital_TPS		**99.3**	**96.6**	**97.2**	**91.1**
	Global				
Sagittal_Cal		**94.9**	**85.0**	**93.4**	**81.5**
	Local				
Pel	**Gamma**	**3%/3mm**	**2mm/3%**	**3mm/2%**	**2mm/2%**
Coronal_TPS		99.9	99.5	99.7	98.6
	Global				
Coronal_Cal	**Local**	**99.5**	**98.4**	**99.1**	**96.6**

Transverse_TPS		**99.9**	**99.4**	**98.6**	**95.0**
	Global				
Transverse_Cal		**99.2**	**95.1**	**97.2**	**89.9**
	Local				
Saggital_TPS		**99.8**	**98.8**	**98.7**	**95.0**
	Global				
Sagittal_Cal		**98.2**	**92.6**	**96.3**	**87.5**
	Local				
Thorax	**Gamma**	**3%/3mm**	**2mm/3%**	**3mm/2%**	**2mm/2%**
Coronal_TPS	**Global**	**99.1**	**96.8**	**98.0**	**94.4**

		3%/3mm	2mm/3%	3mm/2%	2mm/2%
Coronal_Cal		98.8	96.0	97.6	93.4
	Local				
Transverse_TPS		99.7	98.1	98.2	94.0
	Global				
Transverse_Cal		96.2	87.4	94.0	82.6
	Local				
Saggital_TPS		99.7	98.9	98.9	95.2
	Global				
Sagittal_Cal		94.9	85.0	93.4	81.5
	Local				
Brain	Gamma	3%/3mm	2mm/3%	3mm/2%	2mm/2%
Coronal_TPS	Global	99.8	98.3	99.3	95.9

		3%/3 mm	2%/3 mm	3%/2 mm	2%/2 mm
Coronal_Cal		98.9	95.2	98.1	91.9
Transverse_TPS	**Local**	99.4	97.3	98.1	93.8
Transverse_Cal	**Global**	97.8	91.8	96.6	88.2
Saggital_TPS	**Local**	99.6	97.4	98.5	94.2
Sagittal_Cal	**Global**	98.6	93.8	97.7	90.8
	Local				

Supplementary Figures: The figures above illustrate the results of gamma evaluations comparing measured and calculated dose maps for various global and local criteria (DD, DTA; 3%/3 mm, 2%/3 mm, 3%/2 mm, and 2%/2 mm) across different anatomical regions: Brain, Head and Neck, Thorax, and Pelvis. These evaluations were performed on Coronal,

Sagittal, and Transverse cross-sectional views. The data indicate that the maximum failure rate varies depending on the specific gamma criteria and cross-sectional view. Notably, a majority of the failed points are situated at the field edge or in areas where the target and organs at risk overlap. As we move towards stricter gamma criteria, a higher number of failed points are observed, primarily originating from regions with low-dose levels. Furthermore, both global and local gamma evaluations, the 2 mm/3% gamma criteria are more stringent compared to the 3 mm/2% criteria across all the mentioned anatomical sites